

## Effect of pH, Initial Concentration, Background Electrolyte, and Ionic Strength on Cadmium Adsorption by TiO<sub>2</sub> and $\gamma$ -Al<sub>2</sub>O<sub>3</sub> Nanoparticles

Shirzadeh, M., Sepehr, E.,\* Rasouli Sadaghiani, M. H. and Ahmadi, F.

Soil Science Department, Faculty of Agriculture, Urmia University, P.O.Box 57159-44931, Urmia, Iran

Received: 03.08.2019

Accepted: 03.12.2019

**ABSTRACT :** The entrance of Cd (II) to aqueous environments causes a major problem to human health. The current article examines the efficiency of TiO<sub>2</sub> and  $\gamma$ -Al<sub>2</sub>O<sub>3</sub> nanoparticles in Cd (II) removal from aqueous medium as influenced by different chemical factors, such as pH, initial concentration, background electrolyte, and ionic strength, in accordance with standard experimental methods. It conducts Batch experiments, fitting various isotherm models (Freundlich, Langmuir, Temkin, and Dubinin-Radushkevich) to the equilibrium data. Saturation indices (SI) of TiO<sub>2</sub> and  $\gamma$ -Al<sub>2</sub>O<sub>3</sub> nanosorbents indicate that adsorption is a predominant mechanism for Cd (II) removal from aqueous solution, giving maximum Cd (II) adsorption rates of 3348 and 1173 mg/kg for TiO<sub>2</sub> and  $\gamma$ -Al<sub>2</sub>O<sub>3</sub> nanoparticles, respectively, both obtained at the highest pH level (pH = 8) as well as the highest initial Cd (II) concentration (equal to 80 mg/L). Cadmium removal efficiency with TiO<sub>2</sub> and  $\gamma$ -Al<sub>2</sub>O<sub>3</sub> nanoparticles has increased by raising pH from 6 to 8. The Freundlich adsorption isotherm model could fit the experimental equilibrium data well at different pH levels. Also, it has been revealed that cadmium adsorption drops as the ionic strength is increased. The maximum Cd (II) adsorption (1625 mg/kg) has been attained at 0.01 M ionic strength in the presence of NaCl. Thermodynamic calculations demonstrate the spontaneous nature of Cd (II) adsorption by TiO<sub>2</sub> and  $\gamma$ -Al<sub>2</sub>O<sub>3</sub> nanoparticles. The former (TiO<sub>2</sub>) have high adsorption capacities, suggesting they are probably effective metal sorbents, compared to the latter ( $\gamma$ -Al<sub>2</sub>O<sub>3</sub>).

**Keywords:** Cadmium adsorption, Isotherm models, Removal efficiency, Speciation, Visual MINTEQ.

### INTRODUCTION

Cadmium (Cd (II)) as one of the chemical pollutants in the surrounding environment, due to its non-degradable, immanent and accumulative essence even when present in trace concentrations, has engrossed a lot of attentions from past to recent (Tabesh et al., 2018; Kataria & Garg, 2018; Parvin et al., 2019). Cadmium pollution was considered as a serious problem for human

health because it can introduce to the food chain from contaminated environments (Chen et al., 2017; Lin et al., 2018). The International Agency for Research of Cancer (IARC, 1974) classified the Cd (II) as toxic and carcinogenic heavy metal to human health. The efficiency of various body organs of living species are affected by Cd (II), and different drastic and torrid diseases also cause by Cd (II) exposure (Chen et al., 2017). The maximum acceptable levels of Cd (II) in drinking

\*Corresponding Author, Email: [e.sepehr@urmia.ac.ir](mailto:e.sepehr@urmia.ac.ir)

water are 0.003 mg/ L and 0.005 mg/ L according to WHO (2011) and USEPR (2012) respectively. Thus, it is very necessary to specify effective methods for control of Cd pollution and increase environmental protection.

Modern technologies have been expanded for decreasing heavy metals concentration from the environment. Several technologies including precipitation (Fan et al., 2017), advance oxidation (Cheng et al., 2016), flocculation (Folens et al., 2017), electrolysis (Li et al., 2016), adsorption (Yu et al., 2018; Vilarde et al., 2018; Sharma et al., 2019), ion exchange and membrane technology (Lu et al., 2018). However, most of these technologies are usually inconclusive and costly, because of diffusion restriction or the deficit of adequate active surface sites of them, particularly when the heavy metal concentration exceeds of 100 ppm (Koju et al., 2018; Haq et al., 2019). Regarding all various technologies, adsorption is considered as a quick, simple, environmentally friendly, useful, economical and worldwide method. The nature of the adsorbent and efficient parameters for removal of metal from the aqueous and non-aqueous environments are important agents for the increase of adsorptive separation efficiency (Sharma et al., 2019).

Recently, success achievements in nanotechnology result in attention to produce novel nanoadsorbents for heavy metals removal from solutions. Several adsorbents including MgO nanoparticles (Lu et al., 2018; Parvin et al., 2019), magnetic biosorbent (Bonilla-Petriciolet et al., 2018), and Fe<sub>2</sub>O<sub>3</sub> nanoparticles (Li et al., 2019) have been applied for removal of various heavy metals from aqueous solution. Because of nanoadsorbents unique physical and chemical properties, and high- performance specific surface area, there is great consideration to these adsorbents recently (Bashir et al., 2018; Musso et al., 2019; Sharma et al., 2019). If different metal oxides supplied and

activated correctly, they can use as adsorbents. High consistency, appropriate dielectric properties and photocatalytic activity of TiO<sub>2</sub> lead to acceptable performance of this nanoparticle as an adsorbent (Lajayer et al., 2018), also,  $\gamma$ -Al<sub>2</sub>O<sub>3</sub> nanoparticles has potentially high resistance to chemical factors, So the nanoparticles are capable of acting as a catalyst in different chemical reactions (Gatabi et al., 2016; Lu et al., 2018).

Although there are many previous reports about the removal of Cd (II) in the aqueous medium, there is little prior research on Cd (II) removal affected by different background electrolytes with various ionic strengths. So the basic goal of this study was to assess the efficiency of two common nanoparticles (TiO<sub>2</sub> and  $\gamma$ -Al<sub>2</sub>O<sub>3</sub>) in Cd (II) removal from solution, also the influence of pH, Cd (II) initial concentrations and background electrolyte with different ionic strengths factors on Cd (II) adsorption by various nanoparticles were identified in this study.

## MATERIAL & METHODS

Nanostructured TiO<sub>2</sub> and  $\gamma$ -Al<sub>2</sub>O<sub>3</sub> were analytical grade and used without further impurity (purity, 99%) from Nanopars Lima (www. Nanopars Lima co, Iran). Nanoparticles shape and morphology were recognized by using Scanning electron microscope X-ray (Genesis XM2, USA). BET- nitrogen gas (Brunauer-Emmett-Teller) analysis was performed for determining the specific surface area of nanoadsorbents (Quantachrome Nova 2000e, USA) at 77.4 K. Speciation

The Cd speciation and saturation indices (SI) in isotherm supernatants at the latest concentration (80 mg/ L) were computed using the chemical equilibrium model Visual MINTEQ version .3.1. Visual MINTEQ is a geochemical model to identify the metal speciation, solubility equilibria, etc. of natural or laboratory solutions (Allison et al., 1991). The saturation index (SI) is calculated

from the difference between the logarithm of the ion activity product (log IAP) and, the logarithm of the temperature corrected solubility constant (log  $K_s$ ) for each solid compound of the experiment. Over-saturation, under-saturation and equilibrium conditions with the solid phase are occurred when  $SI > 0$ ,  $SI < 0$ , and  $SI = 0$  (or more accurately,  $-0.5 < SI < 0.5$ ) respectively (Allison et al, 1991).

A batch adsorption isotherm experiment was carried out using  $Cd^{2+}$  solutions at different initial concentrations (0, 2.5, 5, 10, 20, 40, and 80 mg/ L) at  $25 \pm 1^\circ C$ , with 0.1 g nanostructured materials and 5 mL of adsorbate at different concentrations. The background solution was 0.01 M sodium nitrate ( $NaNO_3$ ) in order to neutralization of ionic strength, due to less competition of  $Na^+$  ions with  $Cd^{2+}$  for active adsorption sites of minerals, mainly in low concentrations (Bhardwaj et al., 2019). Adjustment of pH was accomplished using either 1 N NaOH or 1 N HCl. Samples were shaken for 2 h (1000 rpm) and left for 24 h at room temperature for equilibration. The concentration of Cd (II) in solutions was measured by Flame Atomic Adsorption Spectrophotometer (AAS, Shimadzu AA- 6300, Japan) after separation of solid-liquid phases of nanoparticle suspensions by centrifugation for 30 min (10000 rpm) and filtered through No. 42 Whatman filter paper. All expressed adsorption experimental data were navigated as the mean of three replicates with less than 5% standard deviation. Cadmium removal efficiency (%) was calculated by the following equation (Kataria & Garg, 2018):

$$\text{Removal Efficiency}(\%) = (C_0 - C_e) / C_0 \times 100 \quad (1)$$

where  $C_0$  (mg/L) and  $C_e$  (mg/ L) are the initial and equilibrium Cd (II) concentrations respectively.

The Freundlich empirical equation, especially for founding the monotonous energy distribution and the heterogeneity of the sorbent surface, is expressed as (Freundlich, 1906):

$$Q_m = K_F \times C_e^{\left(\frac{1}{n}\right)} \quad (2)$$

where  $Q_m$  is the amount of metal ion adsorbed (mg/ kg),  $K_F$  is the Freundlich constant representing the adsorption capacity (L/ mg),  $C_e$  is metal equilibrium concentration (mg/ L), and the adsorption intensity was expressed by  $n$  as a constant value (dimensionless). The Langmuir equation is intended for a homogeneous surface of the adsorbent, is described as (Langmuir, 1916):

$$Q_m = (K_L \times C_e \times S_m) / (1 + K_L \times C_e) \quad (3)$$

where  $Q_m$  and  $C_e$  have the same definitions as in Equation (3),  $K_L$  is a constant of the Langmuir equation, that is related to adsorption affiliation of binding sites for ion adsorption (L/mg), and  $S_m$  is the maximum adsorption capacity with monolayer coverage (mg/ kg).

The Temkin equation that is leaning of the linear decrement of adsorption energy due to adsorbent/ adsorbate interactions is represented as (Temkin & Pyzhev, 1940):

$$Q_m = A + K_T \times \ln(C_e) \quad (4)$$

where  $Q_m$  and  $C_e$  are the same as above mentioned,  $A$  is the constant and intercept of equation (L/g), and  $K_T$  is the constant value of the Temkin equation that is represented the sorption heat (J/ mol).

The adsorption mechanism was usually expressed by using Dubinin–Radushkevich equation that is related to Gaussian energy distribution onto a heterogeneous surface. It can be expressed as Dubinin-Radushkevich (Dubinin, 1960):

$$Q_m = q_{DR} \exp(-\beta_{DR} \times \varepsilon_{DR}^2) \quad (5)$$

where  $Q_m$  is the adsorbed ion amount per unit weight (mmol/g),  $q_{DR}$  (mmol/ g) and  $\beta_{DR}$  ( $mol^2/ J^2$ ) are the empirical constants of the equation and  $\varepsilon_{DR}$  is related to the Polanyi potential that expressed as  $RT \ln(1 + (1/C_e))$ , where  $R$  and  $T$  are the gas constant (8.314 J/ mol. K) and absolute temperature (K)

respectively. The adsorption free energy ( $E$ ) generally is related to the value of  $\beta_{DR}$  that can be computed from the following equation (Dubinin, 1960):

$$E = 1/\sqrt{2\beta_{DR}} \quad (6)$$

The type of adsorption mechanism is related to adsorption free energy (kJ/ mol). Physisorption, ion exchange and chemisorption mechanisms have adsorption energy in the range of 1-8 kJ/ mol, 8- 16 kJ/ mol, and 20-40 kJ/ mol respectively.

Different concentrations (0.01, 0.1, and 0.5 M) of chloride salts (CaCl<sub>2</sub> and NaCl) were added to 5 mL of 80 mg/ L Cd (II) solution with 0.1 g nanoparticles. The pH of each sample was monitored at the end of each experiment to verify any changes which were statistically negligible. The suspensions were shaken for 2 h and left overnight for equilibration. Equilibrium Cd (II) concentration in solution samples were measured by Atomic Adsorption Spectrophotometer, after centrifuging at 10000 rpm for 30 min (Sharma et al., 2019).

Adsorption of Cd (II) onto nanoadsorbents base on thermodynamic studies was calculated at constant temperature (298 K). The probability of spontaneous adsorption was determined by the thermodynamic parameter such as Gibb's free energy ( $\Delta G^0$ ). The parameter was calculated by the following equation (Vilardi et al., 2018):

$$\Delta G^0 = -RT \ln(K_L \times 10^6) \quad (7)$$

where  $R$ ,  $T$  and  $K_L$  are commonly gas constant (8.314 J/ mol K), absolute temperature (K), and the constant of the Langmuir equation (dimensionless, due to multiple at  $10^6$ ) respectively. The Arrhenius equation was used to determine kinetic of adsorption reactions. It can be expressed as the following equation (Laidler, 1984):

$$K(T) = (K_B \times T/h \times C_0) \exp^{-\Delta G^0/RT} \quad (8)$$

$K_B$  is the Boltzmann constant ( $1.380 \times 10^{-23}$

J/ K),  $T$  is the absolute temperature (K),  $h$  is the plank constant ( $6.626 \times 10^{-34}$  J/S),  $C_0$  is the concentration (mol/ L),  $R$  is the gas constant (8.314 J/ mol K), and  $\Delta G^0$  is Gibb's free energy (KJ/ mol) respectively.

The coefficient of determination ( $R^2$ ) and the root mean square error (RMSE) statistics were used to evaluate the goodness of fit and absolute error measures respectively. The RMSE is expressed as (Wang et al., 2019):

$$RMSE = \sqrt{\sum_{i=1}^n (P_i - O_i)^2 / n} \quad (9)$$

where  $P_i$  and  $O_i$  are the predicted and measured values of Cd (II) concentrations sorbed to nanoadsorbents and  $n$  is the number of initial Cd (II) concentrations applied in sorption experiment respectively. Root mean square error (0 to  $+\infty$ ) was used as an index of absolute error. A lower RMSE and higher  $R^2$  values show better goodness of fit between measured and estimated data.

Statistical evaluation was performed using SAS 9.3 (SAS Institute, 2011), speciation of Cd (II) in aqueous was accomplished by Visual MINTEQ 3.1, and bar chart, line graphs and surface plot were drawn using Microsoft Office Excel 2015 software. Optimization of various parameters of adsorption models were performed using Solver 2015.

## RESULTS AND DISCUSSION

The mean diameters of TiO<sub>2</sub> and  $\gamma$ -Al<sub>2</sub>O<sub>3</sub> nanoparticles were 10 nm and 20 nm respectively and both nanoparticles showed the spherical shape prior to adsorption (Fig. 1). Based on nanoadsorbents SEM images, although TiO<sub>2</sub> nanoparticles were homogeneous in size,  $\gamma$ -Al<sub>2</sub>O<sub>3</sub> nanosorbents showed a high surface homogeneity. The BET equation was applied to calculate the specific surface area of nanomaterials. According to results, the TiO<sub>2</sub> nanoparticles had a greater surface area (200 m<sup>2</sup>/g) than  $\gamma$ -Al<sub>2</sub>O<sub>3</sub> (150

m<sup>2</sup>/g). Nanoparticles diameter and specific surface area significantly affect the adsorption capacity (Lajayer et al., 2018).

Metal speciation in solution results from competition between different metal complexes, metal chelates, and free metal ions. Table 1 shows the frequencies of various Cd species at different pH with TiO<sub>2</sub> and γ-Al<sub>2</sub>O<sub>3</sub> nanosorbents. Free metal ions (Cd<sup>2+</sup>) were predominant in solutions with two nanoparticles at different pH, but the proportion of other Cd species were negligible. Several studies showed that the

prominent chemical form of Cd was Cd<sup>2+</sup> in pH ranging from 6 to 8 (Koju et al., 2018; Haq et al., 2019; Li et al., 2019).

Saturation indices of different Cd<sup>2+</sup> minerals were all below zero and undersaturated in solutions with TiO<sub>2</sub> and γ-Al<sub>2</sub>O<sub>3</sub> nanoparticles at various pH (Table 2). According to geochemical modeling data, no precipitation was occur in solution with the nanoparticles (Table 2). So the physical adsorption on nanoparticle surfaces was the predominant mechanism for Cd (II) removal from aqueous solution.

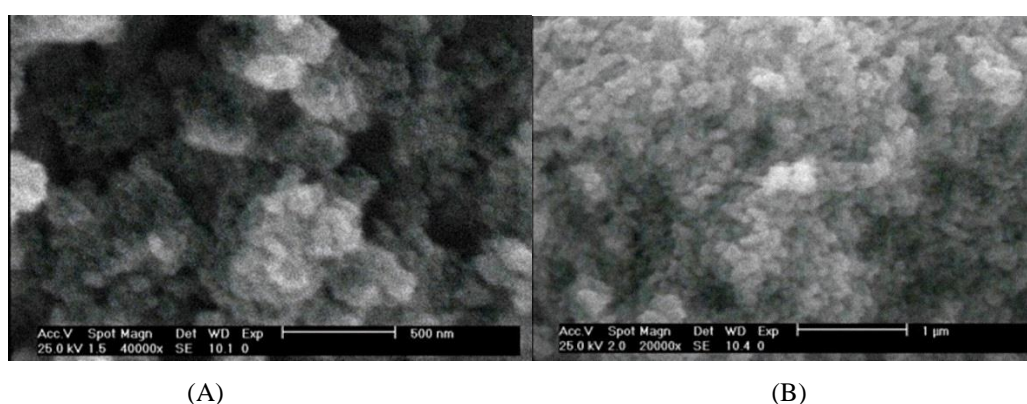


Fig. 1. SEM images of (A) TiO<sub>2</sub>, (B) Al<sub>2</sub>O<sub>3</sub> nanoparticles

Table 1. Speciation of Cd in equilibrium solution in contact with the nanoparticles at different pH using Visual MINTEQ model (Ionic strength 0.01M Na (NO<sub>3</sub>))

Species	Frequency (%)		
	pH 6	pH 7	pH 8
Cd <sup>2+</sup>	98.4	98.0	97.9
Cd (NO <sub>3</sub> ) <sup>+</sup>	1.5	1.9	2.1
Cd (OH) <sub>2</sub>	0.05	0.07	0.4
Cd (OH) <sup>+</sup>	0.02	1.2	1.3
CdCl <sup>+</sup>	1.4	1.8	2.4

Table 2. Saturation indices of minerals in equilibrium solution in contact with nanoparticles at different pH using Visual MINTEQ (Ionic strength 0.01M Na (NO<sub>3</sub>))

Adsorbent	Cd minerals	pH 6	pH 7	pH 8
TiO <sub>2</sub>	Cd (OH) <sub>2</sub>	-2.4	-1.3	-1.4
	Cd (NO <sub>3</sub> ) <sub>2</sub>	-1.5	-2.5	-1.2
	Lime	-22.9	-20.4	-18.3
	Portlandite	-12.9	-10.2	-8.9
γ-Al <sub>2</sub> O <sub>3</sub>	Cd (OH) <sub>2</sub>	-5.0	-2.8	-1.0
	Al (OH) <sub>3</sub>	-1.5	-2.3	-1.1
	Boehmite	-1.2	-3.4	-2.6
	Diaspore	-2.9	-1.2	-1.2
	Lime	-22.9	-20.5	-18.9
	Portlandite	-12.9	-8.7	-8.9

The adsorption capacity of  $\text{TiO}_2$  and  $\gamma\text{-Al}_2\text{O}_3$  nanoparticles was evaluated at various initial concentrations. As can be seen in Fig. 2, the adsorption capacity of Cd (II) continuously increased with the increase of equilibrium concentration at different pH. Increasing of Cd (II) adsorption with nano-oxides was attributed to the pH-dependent charge of these adsorbents (Chen et al., 2017; Tabesh et al., 2018). Electrostatic repulsion between positively charge Cd (II) ions and positively nanoparticle surfaces generated at the pH less than  $\text{pH}_{\text{ZPC}}$ , causes to diminish the adsorption of Cd ions as outer sphere complexes (Razzaz et al., 2016). However, inner sphere complexes are responsible for metal adsorption at  $\text{pH} > \text{pH}_{\text{ZPC}}$ .

In order to determine the maximum Cd (II) adsorption and adsorption parameters, four equilibrium models were fitted to the experimental data, including Freundlich, Langmuir, Temkin, and Dubinin Radushkevich equations (Tables 3 and 4). By

comparing the statistical parameters, it was found that the Freundlich model could well fit the experimental equilibrium data at different pH (Table 3). This indicated the surface heterogeneity of nanoparticles, uniform energy distribution and reversible Cd (II) adsorption during the sorption process.

Adsorption parameters of the Langmuir model indicated the maximum Cd (II) adsorption capacity ( $S_m$ ) with  $\text{TiO}_2$  nanoparticles was 2733, 2981, and 3348 mg/kg at pH 6, 7, and 8 respectively. For  $\gamma\text{-Al}_2\text{O}_3$  the maximum adsorption capacity was in the following order: 1173 mg/kg (pH 8) > 918 mg/kg (pH 7) > 368 mg/kg (pH 6). Comparing of the results with various previous studies shows that experimental data of the present study was found to be lower than those of many corresponding nanosorbents in the literatures (Islam et al., 2018; Szatyłowicz et al., 2018; Wang et al., 2019).

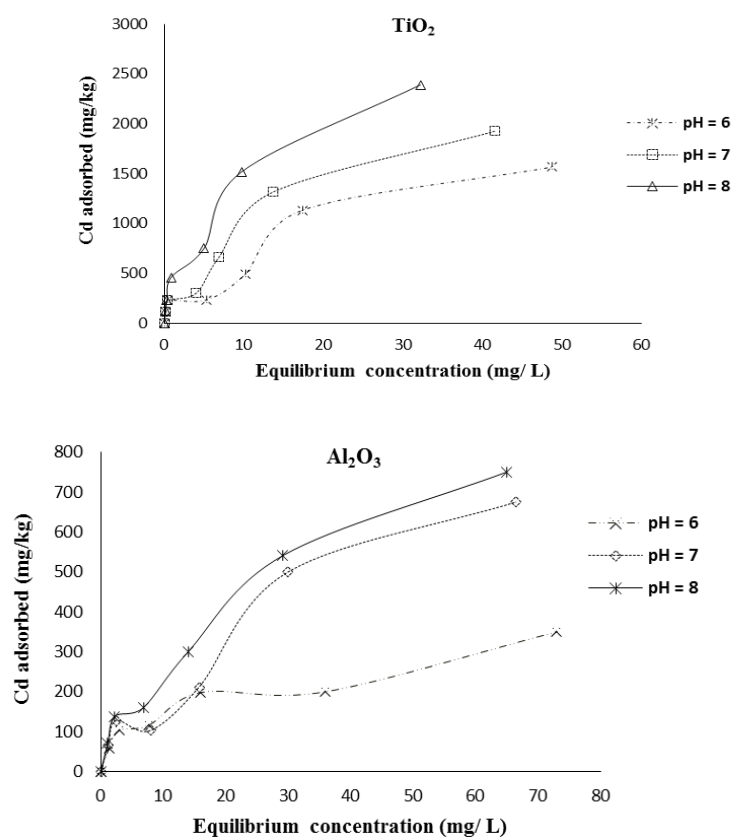


Fig. 2. Effect of pH on Cd (II) adsorption by nanoadsorbents

The Dubinin Radushkevich equation was fitted to specify the chemical or physical adsorption mechanisms. The adsorption free energy of the Dubinin Radushkevich equation was less than 8 kJ/mol with both nanoparticles at different pH which is evidence of physically adsorption mechanism of Cd (II) onto nanoparticle surface (Table 3). In physical adsorption, the individuality of the

adsorbate and the adsorbent are preserved. In return, chemisorption occurs as a chemical reaction between the adsorbate and the surface. Also new chemical bonds are generated at the adsorbent surface (Rahmani et al., 2010). The Temkin model failed to fit the Cd (II) isotherms with both studied nanoadsorbents in compare with other isotherm models (Table 3).

**Table 3. Isotherm equation parameters for adsorption of Cd (II) by TiO<sub>2</sub> and γ-Al<sub>2</sub>O<sub>3</sub> nanoparticles**

Adsorbent	pH	Freundlich				Langmuir				Temkin				Dubinin-Radushkevich				
		K <sub>F</sub>	n	R <sup>2</sup>	RMSE	S <sub>m</sub>	K <sub>L</sub>	R <sup>2</sup>	RMSE	A	K <sub>T</sub>	R <sup>2</sup>	RMSE	q <sub>DR</sub>	β <sub>DR</sub>	E	R <sup>2</sup>	RMSE
		(L/mg <sup>1/n</sup> )				(mg/kg)	(L/mg)			(L)	(mg/L)		(mg/mg)	(L <sup>2</sup> /mg <sup>2</sup> )	(kJ)			
TiO <sub>2</sub>	6	154	1.65	0.95	0.04	2733	0.02	0.95	0.13	270	243	0.85	0.22	0.010	2.02 × 10 <sup>-5</sup>	1.57	0.93	0.18
	7	242	1.77	0.95	0.06	2981	0.04	0.97	0.11	407	298	0.77	0.32	0.002	7.15 × 10 <sup>-4</sup>	2.64	0.94	0.15
	8	425	1.99	0.98	0.08	3348	0.07	0.94	0.36	657	382	0.86	0.65	0.002	6.33 × 10 <sup>-6</sup>	4.32	0.92	0.39
γ-Al <sub>2</sub> O <sub>3</sub>	6	53	1.35	0.95	0.01	368	0.06	0.90	0.08	20.83	64	0.90	0.03	0.002	1.71 × 10 <sup>-5</sup>	1.70	0.92	0.08
	7	58	1.50	0.95	0.03	918	0.08	0.91	0.07	15.31	130	0.88	0.08	0.006	2.03 × 10 <sup>-5</sup>	1.56	0.95	0.05
	8	69	1.73	0.98	0.03	1173	0.11	0.96	0.03	7.62	153	0.92	0.07	0.006	2.63 × 10 <sup>-5</sup>	1.37	0.92	0.02

K<sub>F</sub> is the Freundlich equation constant; n is the empirical constant of the Freundlich equation; S<sub>m</sub> is maximum adsorption capacity; K<sub>L</sub> is the Langmuir equation constant; A is the empirical constant; K<sub>T</sub> is the constant value of the Temkin equation; q<sub>DR</sub> and β<sub>DR</sub> are the empirical Dubinin-Radushkevich equation constants; and E is the adsorption free energy.

**Table 4. Cadmium adsorption capacity by TiO<sub>2</sub> and γ-Al<sub>2</sub>O<sub>3</sub> nanoparticles at different pH**

Adsorbent	pH	Freundlich		Langmuir		Temkin		Dubinin-Radushkevich	
		Q <sub>e</sub>	Q <sub>m</sub>	Q <sub>e</sub>	Q <sub>m</sub>	Q <sub>e</sub>	Q <sub>m</sub>	Q <sub>e</sub>	Q <sub>m</sub>
		(mg/kg)		(mg/kg)		(mg/kg)		(mg/kg)	
TiO <sub>2</sub>	6	1566	1615	1566	1607	1566	1214	1566	1650
	7	1925	1984	1925	1962	1925	1518	1925	1930
	8	2391	2422	2391	2392	2391	1985	2391	2310
γ-Al <sub>2</sub> O <sub>3</sub>	6	350	559	350	307	350	295	350	290
	7	675	950	675	781	675	561	675	693
	8	750	769	750	1037	750	650	750	710

Q<sub>e</sub> and Q<sub>m</sub> are the maximum equilibrium Cd (II) concentration and predicted by the model respectively.

Cadmium removal from solution increased as the initial pH increased from 6 to 8 for both nanoparticles (Fig. 3). The significant low removal efficiency at pH 6 for TiO<sub>2</sub> (54 %) and γ-Al<sub>2</sub>O<sub>3</sub> (25%) nanoparticles can be related to the fact that in lower pH medium, nanoparticles has the predominance of positive charges on their surface due to their high pHzpc 6.9 (TiO<sub>2</sub>) and 7.2 (γ-Al<sub>2</sub>O<sub>3</sub>) and the high electrostatic repelling forces inhibits the contact of Cd<sup>2+</sup> and the nanoparticles surface (Saleh et al., 2016; Vilardi et al., 2018). Same results were found by Song et al (2011) and Huang

et al (2016). A continuous increase in removal efficiency was found by increasing the pH range from 6 to 8. Previous studies have shown that pH of 7–7.5 was optimum for Cd<sup>2+</sup> adsorption on TiO<sub>2</sub> and γ-Al<sub>2</sub>O<sub>3</sub> nanoparticles (Tabesh et al., 2018; Sharma et al., 2019). Obtained results showed the significant differences in Cd (II) removal efficiency with TiO<sub>2</sub> and γ-Al<sub>2</sub>O<sub>3</sub> nanoparticles at different pH (Fig. 3). Higher surface area and specific adsorption sites are effective to increase nanoparticles ability to heavy metals removal from aqueous solution (Saleh et al., 2016).

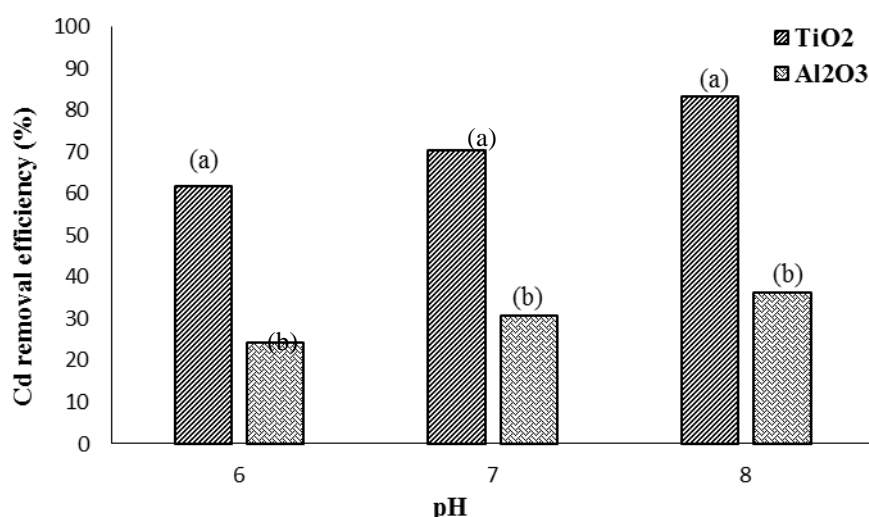


Fig. 3. Effect of pH on Cd (II) removal efficiency with TiO<sub>2</sub> and Al<sub>2</sub>O<sub>3</sub> nanoparticles

\*Same letters indicate no significant difference at the  $\alpha < 5\%$  level (The comparison between the removal efficiency of each nanoparticle in a given pH is done)

As shown in Fig. 4, the amount of Cd (II) adsorbed with both nanoparticles increased significantly by increasing of Cd (II) concentration from 2.5 to 80 mg/ L. The maximum Cd (II) adsorption on TiO<sub>2</sub> and  $\gamma$ -Al<sub>2</sub>O<sub>3</sub> nanoparticles were 2500 mg/kg and 2390 mg/ kg at the highest initial Cd (II) concentration and pH respectively, which is higher than that of many other adsorbents reported in literature (Haq et al., 2019). In this study, optimum initial concentration for Cd (II) adsorption with TiO<sub>2</sub> and  $\gamma$ -Al<sub>2</sub>O<sub>3</sub> nanoparticles cannot be determined exactly, but it is more than 80 mg/L certainly, because Cd (II) adsorption increased up to 80 mg/L continuously by increasing of initial concentration. Various range of optimum initial Cd (II) concentration were reported in other studies (Cheng et al., 2012; Zadeh et al., 2018; Sharififard et al., 2019). More than 200 mg/ L was reported as the optimum initial Cd (II) concentration with TiO<sub>2</sub> nanoparticles (Razzaz et al., 2016). Increasing the initial concentration leads to a strong tensile force between dissolved ions and solid phase, results in increase of adsorption (Huang et al., 2016). However, at higher initial concentrations most of the active sites are occupy which results in

partial deactivation of the nanoparticle surfaces, so available surface sites have decreased that decline the adsorption capacity of nanoadsorbents (Tabesh et al., 2018; Kataria & Garg, 2019). The higher Cd (II) adsorption capacity of TiO<sub>2</sub> nanoparticles in different initial concentrations can be attributed to the lower particle diameter and surface properties of the nanoparticle (El-Deen & Zhang, 2016; Kow et al., 2017). The results are consistent with previous studies (Park et al., 2017; Kim et al., 2019).

The Cd (II) removal efficiency with TiO<sub>2</sub> and  $\gamma$ -Al<sub>2</sub>O<sub>3</sub> nanoparticles as affected by various range of initial Cd (II) concentrations and pH is shown in Fig. 5. The Cd (II) removal efficiency of both nanoparticles was decreased by increasing of initial concentration. The maximum Cd (II) removal efficiency (95%) with TiO<sub>2</sub> was obtained at minimum initial Cd (II) concentration (2.5 mg/ L) at the highest pH. However, the removal efficiency increased by increasing pH from 6 to 8, as the lowest Cd (II) removal efficiency (38%) was obtained at the highest initial concentration and the lowest pH (Fig. 5). Same results were found with  $\gamma$ - Al<sub>2</sub>O<sub>3</sub> nanoparticles as well. The Cd (II) removal



efficiency of  $\gamma\text{-Al}_2\text{O}_3$  at 2.5 mg/ L initial concentration was 46%, 52%, and 56% at pH 6, 7, and 8 respectively. Decreasing the Cd (II) removal efficiency by increasing of initial Cd (II) concentration can be due to the lack of the total amount of available active sites for binding of metal ions onto adsorbents (Kim et al., 2019).

Considering the higher capacity of  $\text{TiO}_2$  nanoparticles in Cd (II) adsorption, the effect of different ionic strengths and background electrolytes on Cd (II) adsorption capacity with the nanoparticle were assessed. As shown in Fig. 6, the Cd (II) adsorption was decreased as increasing

of ionic strength from 0.01 to 0.5 M at a constant pH, indicating competitive adsorption between the background cations and Cd (II) (Fig. 6). Several studies have been reported the reverse effect of ionic strength on Cd (II) adsorption (Tajali Rad et al., 2019; Wang et al., 2019). The effect of ionic strength on electrostatic potential and the maximum adsorption is demonstrated by previous researches (Li et al., 2019; Musso et al., 2019). Negatively charges on surface nano oxides and zeta potential increase by increasing of ionic strength which decrease the adsorption capacity (Bashir et al., 2018).

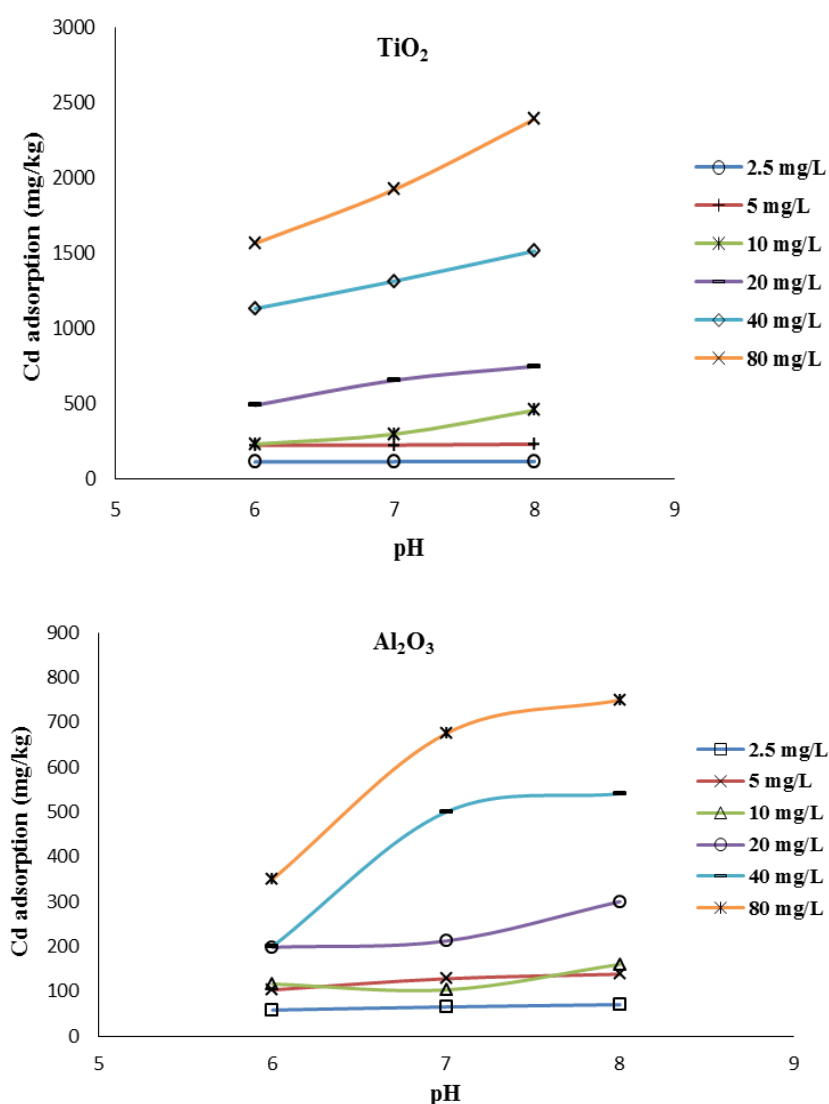


**Fig. 4. Effect of different Cd (II) initial concentration on adsorption**

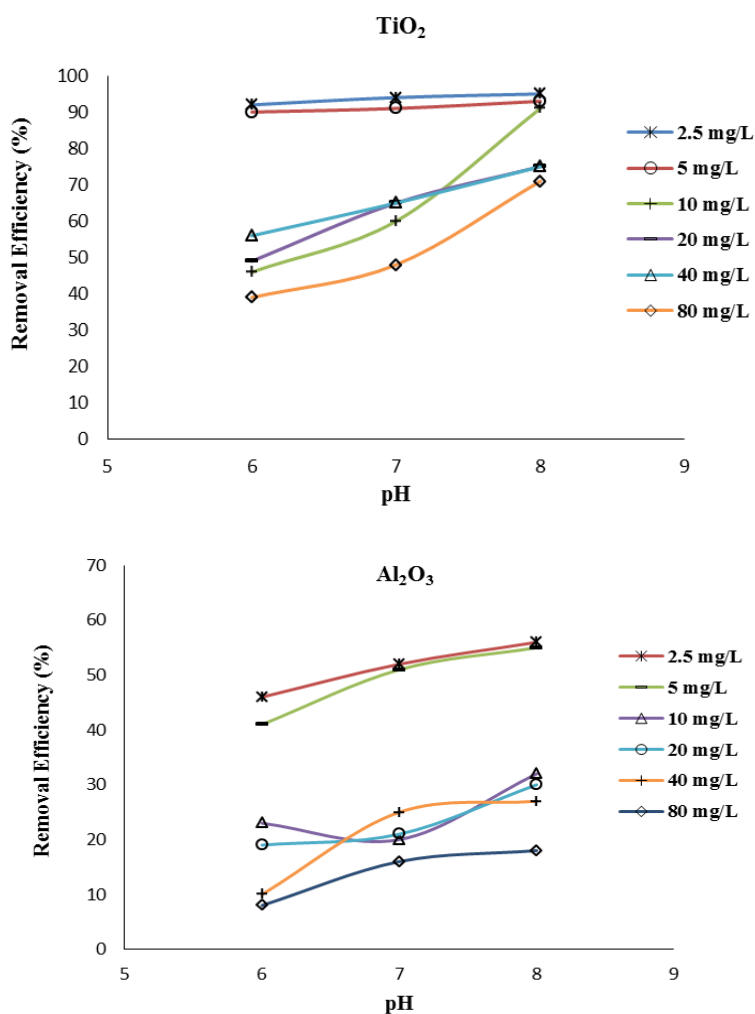


Fig. 5. Effect of Cd (II) initial concentration on removal efficiency

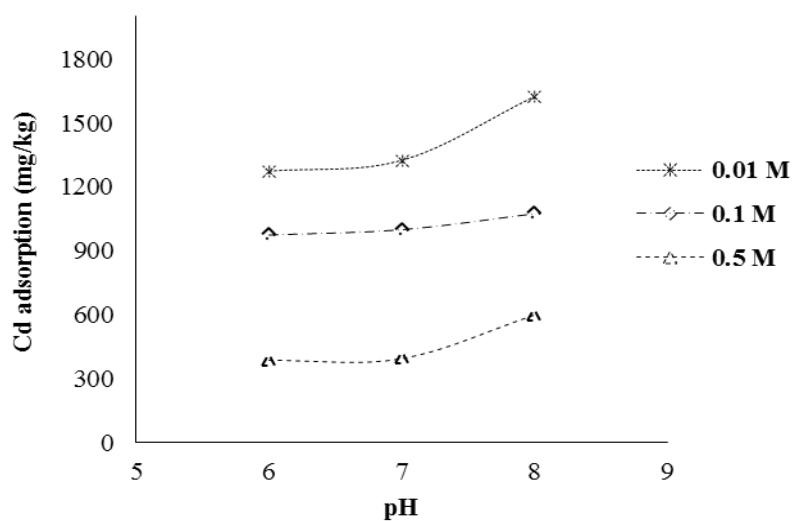


Fig. 6. Effect of ionic strength on Cd adsorption with TiO<sub>2</sub> nanoparticles

Presence of different ions in solution affects the surface charge of nanoparticles and results in the variation of the adsorption (Bonilla-Petriciolet et al., 2018). The competitive effect of some ions on Cd (II) adsorption with TiO<sub>2</sub> nanoparticles was investigated in presence of CaCl<sub>2</sub> and NaCl as various background electrolytes at a constant ionic strength (0.01 M). It is found that the Cd (II) adsorption ranged from

1225 to 1500 mg/ kg and 1275 to 1625 mg/ kg in presence of CaCl<sub>2</sub> and NaCl respectively (Table 5). This may be due to the higher competition of Ca<sup>2+</sup> ions with Cd (II) for adsorption on active surface sites. The results of Li et al. (2016) showed the significant decrease of Cd (II) adsorption using various nanoparticles by increasing of Ca<sup>2+</sup> concentration in solution.

**Table 5. Cadmium adsorption (mg/kg) in presence of 0.01 M CaCl<sub>2</sub> and NaCl as background electrolytes with TiO<sub>2</sub> nanoparticles**

Electrolyte	pH	Cd adsorption (mg/ kg)	Mean adsorption (mg/ kg)
CaCl <sub>2</sub>	6	1225	1400
	7	1475	
	8	1500	
NaCl	6	1275	1408
	7	1325	
	8	1625	

Thermodynamics was studied to determine spontaneous nature of Cd (II) adsorption by nanoparticles at different pH. The Gibbs's free energy ( $\Delta G^0$ ) has been calculated in constant temperature (25 °C) and pressure using thermodynamic relationship. Gibbs's free energy of Cd (II) adsorption reaction with TiO<sub>2</sub> nanoparticles were -25.48, -26.62, and -27.90 kJ/mol at pH 6, 7, and 8 respectively.

$$\Delta G^0 \text{ (kJ/mol), TiO}_2: 1.81 \times 10^{-51} \text{ (pH 6)} < 2.86 \times 10^{-51} \text{ (pH 7)} < 4.80 \times 10^{-51} \text{ (pH 8)}$$

$$\Delta G^0 \text{ (kJ/mol), } \gamma\text{-Al}_2\text{O}_3: 3.70 \times 10^{-51} \text{ (pH 6)} < 4.91 \times 10^{-51} \text{ (pH 7)} < 6.64 \times 10^{-51} \text{ (pH 8)}$$

The kinetic of adsorption reactions increased by increasing pH with both nanoparticles. It can be mentioned that the spontaneous adsorption reactions occur slowly at the lowest pH than the highest.

### CONCLUSION

Experimental studies revealed that TiO<sub>2</sub> and  $\gamma$ -Al<sub>2</sub>O<sub>3</sub> nanoparticles have high efficiency in removing of Cd (II) from aqueous solution. The maximum adsorption capacity of TiO<sub>2</sub> nanoparticles was higher than  $\gamma$ -Al<sub>2</sub>O<sub>3</sub>. Modeling study showed that adsorption was the

For  $\gamma$ -Al<sub>2</sub>O<sub>3</sub> the following result was as; -27.57 (pH 6), -27.97 (pH 7) and -28.76 (pH 8). The more negative amounts of  $\Delta G^0$  demonstrated the spontaneous nature of Cd (II) adsorption by nanoparticles and feasibility of the process. The result of kinetic calculation at 298 K shows the following orders with TiO<sub>2</sub> and  $\gamma$ -Al<sub>2</sub>O<sub>3</sub> nanoparticles by increasing pH respectively;

predominant mechanism for removal of Cd (II) from aqueous solution with the nanoparticles. Cadmium adsorption increased with increasing pH and initial Cd (II) concentration. Maximum removal efficiency increased by increasing pH. Cadmium adsorption decreased by increasing of ionic strength. Cadmium adsorption decreased in the presence of 0.01 M CaCl<sub>2</sub> background electrolyte. Thermodynamic results demonstrated the spontaneous nature of Cd (II) adsorption onto TiO<sub>2</sub> and  $\gamma$ -Al<sub>2</sub>O<sub>3</sub> nanoparticles at different pH. TiO<sub>2</sub> nanoparticles have high

adsorption capacities due to their increased surface area, suggesting they may be effective metal sorbents.

## ACKNOWLEDGMENT

The authors are thankful to the Office of Vice Chancellor for Research and Technology, Urmia University.

## REFERENCES

- Allison, J. D., Brown, D. S. and Novo-Gradac, K. J. (1991). MINTEQA2/PRODEFA2, a geochemical assessment model for environmental systems: version 3.0 user's manual. Environmental Research Laboratory, Office of Research and Development, US Environmental Protection Agency.
- Bashir, S., Rizwan, M. S., Salam, A., Fu, Q., Zhu, J., Shaaban, M. and Hu, H. (2018). Cadmium immobilization potential of rice straw-derived biochar, zeolite and rock phosphate: extraction techniques and adsorption mechanism. *J. Phys. Chem.*, 100(5); 727-732.
- Bonilla-Petriciolet, A., Sellaoui, L., Mendoza-Castillo, D. I., Reynel-Avila, H. E. and Lamine, A. B. (2018). A new statistical physics model for the ternary adsorption of  $\text{Cu}^{2+}$ ,  $\text{Cd}^{2+}$  and  $\text{Zn}^{2+}$  ions on bone char: experimental investigation and simulations. *J. Colloid Interface Sci.*, 21(2); 84-89.
- Bhardwaj, A., Chand, P., Pakade, Y. B., Joshi, R. and Sharma, M. (2019). Kinetic and equilibrium studies on adsorption of cadmium from aqueous solution using *Aesculus Indica* seed shell. *Geoderma*, 40(1); 251-262.
- Chen, K., He, J., Li, Y., Cai, X., Zhang, K., Liu, T. and Liu, J. (2017). Removal of cadmium and lead ions from water by sulfonated magnetic nanoparticle adsorbents. *J. Colloid Interface Sci.*, 494 (1); 307-316.
- Cheng, M., Zeng, G., Huang, D., Lai, C., Xu, P., Zhang, C. and Liu, Y. (2016). Hydroxyl radicals based advanced oxidation processes (AOPs) for remediation of soils contaminated with organic compounds: a review. *Chem. Eng. Sci.*, 284 (1); 582-598.
- Dubinin, M.M. (1960). Sorption and structure of active carbons. I. Adsorption of organic vapors, *Zhurnal Fizicheskoi Khimii*. 21 (1); 1351-1362.
- El-Deen, S. E. A. and Zhang, F. S. (2016). Immobilisation of  $\text{TiO}_2$ -nanoparticles on sewage sludge and their adsorption for cadmium removal from aqueous solutions. *J. Exp. Nanosci.*, 11(4); 239-258.
- Fan, H. L., Zhou, S. F., Jiao, W. Z., Qi, G. S. and Liu, Y. Z. (2017). Removal of heavy metal ions by magnetic chitosan nanoparticles prepared continuously via high-gravity reactive precipitation method. *Carbohydr. Polymer.*, 174 (3); 1192-1200.
- Folens, K., Huysman, S., Van Hulle, S. and Du Laing, G. (2017). Chemical and economic optimization of the coagulation-flocculation process for silver removal and recovery from industrial wastewater. *Sep. Purif. Technol.*, 179 (2); 145-151.
- Freundlich, H. M. F. (1906). Over the adsorption in solution. *J. Phys. Chem.*, 57; 1100-1107.
- Gatabi, M. P., Moghaddam, H. M. and Ghorbani, M. (2016). Efficient removal of cadmium using magnetic multiwalled carbon nanotube nanoadsorbents: equilibrium, kinetic, and thermodynamic study. *J. Nanoparticle Res.*, 18(7); 189-195.
- Haq, S., Rehman, W. and Waseem, M. (2019). Adsorption Efficiency of Anatase  $\text{TiO}_2$  Nanoparticles against Cadmium Ions. *J. Inorg Organomet P.*, 29(3): 651-658.
- Huang, Y., Fulton, A. N. and Keller, A. A. (2016). Simultaneous removal of PAHs and metal contaminants from water using magnetic nanoparticle adsorbents. *Sci Total Environ.*, 571 (1); 1029-1036.
- Kataria, N. and Garg, V. K. (2018). Green synthesis of  $\text{Fe}_3\text{O}_4$  nanoparticles loaded sawdust carbon for cadmium (II) removal from water: Regeneration and mechanism. *Chemosphere.*, 208(2); 818-828.
- Koju, N. K., Song, X., Wang, Q., Hu, Z. and Colombo, C. (2018). Cadmium removal from simulated groundwater using alumina nanoparticles: behaviors and mechanisms. *Environ Pollut.*, 240 (1); 255-266.
- Kow, K. W., Kiew, P. L., Yusoff, R. and Abdullah, E. C. (2017). Preliminary evidence for enhanced adsorption of cadmium (II) ions using nano-magnetite aligned in silica gel matrix. *Chem. Eng. Trans.*, 56 (2); 1231-1236.
- Kim, K., Park, M. S., Na, Y., Choi, J., Jenekhe, S. A. and Kim, F. S. (2019). Preparation and application of polystyrene-grafted alumina core-shell nanoparticles for dielectric surface passivation in solution-processed polymer thin film transistors. *Organic Electronics*, 65 (1); 305-310.
- Laidler, K. J. (1984). The development of the Arrhenius equation. *J. Chem. Educ.*, 61(6); 494.
- Lu, F. and Astruc, D. (2018). Nanomaterials for removal of toxic elements from water. *Coordination Chemistry Reviews*, 356 (1); 147-164.

- Lin, J., Su, B., Sun, M., Chen, B. and Chen, Z. (2018). Biosynthesized iron oxide nanoparticles used for optimized removal of cadmium with response surface methodology. *Sci Total Environ.*, 627 (1); 314-321.
- Lajayer, B. A., Najafi, N., Moghiseh, E., Mosaferi, M. and Hadian, J. (2018). Removal of heavy metals ( $\text{Cu}^{2+}$  and  $\text{Cd}^{2+}$ ) from effluent using gamma irradiation, titanium dioxide nanoparticles and methanol. *J. Nano Structure.*, 8(4); 483-496.
- Li, Y., Yang, Z., Chen, Y. and Huang, L. (2019). Adsorption, recovery, and regeneration of Cd by magnetic phosphate nanoparticles. *J. Phys. Chem.*, 24(2); 1-12.
- Langmuir, I. (1916). The constitution and fundamental properties of solids and liquids. Part I. Solids. *Chemosphere.*, 38(11); 2221-2295.
- Islam, M. A., Morton, D. W., Johnson, B. B., Pramanik, B. K., Mainali, B. and Angove, M. J. (2018). Metal ion and contaminant sorption onto aluminium oxide-based materials: a review and future research. *J. Environ. Chem. Eng.*, 25 (2); 35-42.
- Musso, T. B., Parolo, M. E. and Pettinari, G. (2019). pH, Ionic Strength, and Ion Competition Effect on Cd (II) and Ni (II) Sorption by a Na-bentonite Used as Liner Material. *Polish Journal of Environmental Studies*, 28(4); 35-41.
- Parvin, F., Rikta, S. and Tareq, S. M. (2019). Application of Nanomaterials for the Removal of Heavy Metal from Wastewater. *J. Nanotech in Water and Wastewater Treat.*, 34(2); 137-157.
- Rahmani, A., Zavvar Mosavi, H. and Fazli, M. (2010). Effect of nanostructure alumina on adsorption of heavy metals, *Desalination*, 253(2); 94-100.
- Razzaz, A. Ghorban, S. Hosayni, L. Irani, M. and Aliabadi, M. (2016). Chitosan nanofibers functionalized by  $\text{TiO}_2$  nanoparticles for the removal of heavy metal ions. *J. TAIWAN Inst Chem E.*, 58 (2); 333-343.
- Saleh, T. A. (2016). Nanocomposite of carbon nanotubes/silica nanoparticles and their use for adsorption of Pb (II): from surface properties to sorption mechanism. *Desalin Water Treat.*, 57(23); 10730-10744.
- Szatyłowicz, E. and Skoczko, I. (2018). The use of activated alumina and magnetic field for the removal heavy metals from water. *J. Eco Eng.*, 19(3); 53-62.
- Sharma, M., Singh, J., Hazra, S. and Basu, S. (2019). Adsorption of heavy metal ions by mesoporous ZnO and  $\text{TiO}_2$ : Adsorption and kinetic studies. *Microchemical Journal.*, 14 (1); 105-112.
- Sharififard, H., Ghorbanpour, M. and Hosseinirad, S. (2019). Cadmium removal from wastewater using nano-clay/ $\text{TiO}_2$  composite: kinetics, equilibrium and thermodynamic study. *Chemosphere.*, 25(2); 163-169.
- Tajali Rad, F., Kefayati, H. and Shariati, S. (2019). Synthesis of propyl aminopyridine modified magnetite nanoparticles for cadmium (II) adsorption in aqueous solutions. *Sci Total Environ.*, 33(2); 32-40.
- Temkin, M. J. and Pyzhev, V. (1940). Recent modifications to Langmuir isotherms.
- Tabesh, S., Davar, F. and Loghman-Estarki, M. R. (2018). Preparation of  $\gamma\text{-Al}_2\text{O}_3$  nanoparticles using modified sol-gel method and its use for the adsorption of lead and cadmium ions. *J. Alloy Compd.*, 730 (2); 441-449.
- Vilardi, G., Mpouras, T., Dermatas, D. Verdone, N., Polydera, A. and Di Palma, L. (2018). Nanomaterials application for heavy metals recovery from polluted water: The combination of nano zero-valent iron and carbon nanotubes. Competitive adsorption non-linear modeling. *Chemosphere.*, 201 (2); 716-729.
- Wang, F., Yang, W., Cheng, P. Zhang, S., Zhang, S. Jiao, W. and Sun, Y. (2019). Adsorption characteristics of cadmium onto microplastics from aqueous solutions. *Chemosphere.*, 235 (1); 1073-1080.
- Yu, Z., Hao, R., Zhang, L. and Zhu, Y. (2018). Effects of  $\text{TiO}_2$ ,  $\text{SiO}_2$ , Ag and CdTe/CdS quantum dots nanoparticles on toxicity of cadmium towards *Chlamydomonas reinhardtii*. *Ecotoxic and environ safety.*, 156 (1); 75-86.
- Zadeh, B. S., Esmaeili, H. and Foroutan, R. (2018). Cadmium (II) Removal from Aqueous Solution Using Microporous Eggshell: Kinetic and Equilibrium Studies. *Indonesian Chem.*, 18(2); 265-271.

